Specific Proteolysis of Human Plasminogen by a 24 kDa Endopeptidase from a Novel *Chryseobacterium Sp.*†

H. Roger Lijnen,* Berthe Van Hoef, Francesca Ugwu, Désiré Collen, and Ivo Roelants

Center for Molecular and Vascular Biology, University of Leuven, Leuven, Belgium

Received August 27, 1999; Revised Manuscript Received October 25, 1999

ABSTRACT: A novel single polypeptide endopeptidase of 24 kDa (24k-endopeptidase) was purified with a yield of 300−400 μg/L from conditioned medium of a bacterial strain which was identified as a new species in the genus *Chryseobacterium Sp.* on the basis of its 16S rDNA sequence and DNA:DNA hybridizations. The NH_2-terminal amino acid sequence (Val-Ala-Thr-Pro-Asn-Leu-Glu-...) was not found in the availabe databases. The 24k-endopeptidase specifically hydrolyzed the Ser^{441}−Val^{442} peptide bond in human plasmin(ogen), with additional cleavage of the Lys^{78}−Val^{79} and Pro^{447}−Val^{448} peptide bonds, and a secondary cleavage at Lys^{615}−Val^{616}. Thereby, plasminogen is converted into an angiostatin-like fragment containing kringles 1−4 (K1−4) and miniplasminogen (kringle 5 and the serine proteinase domain). The purified K1−4 fragment showed a comparable cytotoxicity toward endothelial cells as the elastase-derived K1−3 fragment (12.7% versus 10.6% at a concentration of 10 μg/mL). Plasminogen, bound to monocytoid THP-1 cells, was also cleaved by the 24k-endopeptidase, resulting in generation of an angiostatin-like fragment and in a decreased capacity to generate cell-associated plasmin following activation by urokinase. The 24k-endopeptidase was not efficiently neutralized by specific inhibitors against the serine, cysteine, aspartic, or matrix metalloproteinase classes of enzymes. In human plasma or serum, however, it induced only very limited plasminogen degradation, apparently due to neutralization of its activity by α_2-macroglobulin. Interaction of this novel 24k-endopeptidase with plasminogen thus yields an angiostatin-like fragment and affects plasmin-mediated cellular proteolytic activity.

Plasminogen, the zymogen of the fibrinolytic system, is converted to the active enzyme plasmin by tissue-type (t-PA) or urokinase-type (u-PA) plasminogen activator (*1*). Plasmin(ogen) not only plays an essential role in the clearance of fibrin from the circulation (*1, 2*) but also is involved in several other biological phenomena, including macrophage recruitment, arterial stenosis, atherosclerosis, aneurysm formation, skin and corneal wound healing, glomerulonephritis, and neovascularization (reviewed in refs *3* and *4*). Human plasminogen is a single-chain glycoprotein of 92 kDa consisting of 791 amino acids, which is converted to plasmin by specific cleavage of the Arg^{561}−Val^{562} peptide bond (*5, 6*). Native (Glu-) plasminogen can be converted to modified forms (Lys-plasminogen) as a result of hydrolysis of the Arg^{68}−Met^{69}, Lys^{77}−Lys^{78}, or Lys^{78}−Val^{79} peptide bonds by plasmin (*7, 8*). Both chains of plasmin (approximately 65 and 25 kDa) are connected by two disulfide bonds, and the active site is located in the 25 kDa COOH-terminal proteinase domain (*5*). The NH_2-terminal domain consists of five kringle structures, of which the lysine-binding sites located in the kringle 1−3 region play a key role in the regulation of fibrinolysis and are also involved in cellular binding of plasminogen (*9, 10*). Angiostatin, a plasminogen fragment containing kringles 1−4, has antiangiogenic properties (*11*); in vitro it inhibits endothelial cell proliferation (*12*−*14*), and in mice in vivo it inhibits primary tumor growth and angiogenesis-dependent metastases (*11, 14, 15*). The exact composition of the active angiostatin fragment as well as the mechanism by which it is generated in vivo is, however, still debated. In the present study, we show that a novel 24 kDa endopeptidase secreted by a novel species of the *Chryseobacterium* genus specifically cleaves human plasminogen, generating an angiostatin-like fragment, and reducing cell-associated plasmin activity.

EXPERIMENTAL PROCEDURES

Proteins and Reagents. Human Glu-plasminogen, plasmin, α_2-antiplasmin, fibrinogen, and tcu-PA[1] (urokinase) were obtained as described elsewhere (*16*). Elastase-derived miniplasminogen was obtained and characterized as described previously (*17*). Murine, canine, rabbit, bovine, and baboon plasminogens were isolated and characterized as described (*16*). Human plasminogen was labeled with ^{125}I using the Iodogen method to a specific radioactivity of 18 μCi/μg. Human α_2-macroglobulin was a kind gift of Dr. F.

† This study was supported by grants from the Flemish Fund for Scientific Research (FWO, Contract G.0138.00) and from the IUAP (Contract P4/34).

* Address correspondence to this author at the Center for Molecular and Vascular Biology, University of Leuven, Campus Gasthuisberg, O & N, Herestraat 49, B-3000 Leuven, Belgium. Tel: 32-16-345775, Fax: 32-16-345990, E-mail: roger.lijnen@med.kuleuven.ac.be.

[1] Abbreviations: K1−4, plasminogen fragment comprising the first four kringles of plasminogen; MAb, monoclonal antibody; SDS−PAGE, sodium dodecyl sulfate−polyacrylamide gel electrophoresis; S-2403, D-pyroGlu-Phe-Lys-*p*-nitroanilide; tcu-PA, two-chain urokinase-type plasminogen activator.

10.1021/bi992014r CCC: $19.00 © 2000 American Chemical Society
Published on Web 12/14/1999

Van Leuven (Center for Human Genetics, University of Leuven, Belgium).

The following inhibitors were purchased: aprotinin (Trasylol) from Bayer (Leverkusen, Germany), 1,10-phenanthroline and PMSF (phenylmethylsulfonyl fluoride) from Sigma Chemie, EDTA from VEL (Leuven, Belgium), NPGB (4-nitrophenyl-4-guanidinobenzoate hydrochloride) from Merck (Darmstadt, Germany), TPCK (tosyl-L-phenylalanine chloromethyl ketone) from Boehringer Mannheim (Mannheim, Germany), leupeptin and pepstatin from Calbiochem-Novabiochem (Nottingham, U.K.). The chromogenic substrates S-2251 and S-2403 were purchased from Chromogenix AB (Antwerp, Belgium); S-2495, S-2518, S-2524, S-2526, and S-2533 were a kind gift of Chromogenix AB (Mölndal, Sweden). Streptokinase was Streptase from Hoechst (Brussels, Belgium). The monoclonal antibodies directed against plasminogen kringle 5 (MAb-42B12), against the kringle 1−3 fragment (MAb-36E6 and MAb-34D3), and against the proteinase domain (MAb-31E9) were characterized previously (*18*).

The human monocytoid cell line THP-1 was obtained from the American Type Culture Collection (Rockville, MD) and grown in RPMI 1640 medium containing 2 mM L-glutamine, 100 units/mL penicillin, and 0.1 mg/mL streptomycin. Viability of cells was monitored by staining with Trypan blue, and cells were counted microscopically.

Citrated human plasma was clotted with thrombin (two subsequent additions to 2 NIH units/mL and incubation at 37 °C for 30 min), followed by centrifugation.

Assays. SDS−PAGE without reduction or after reduction with 1% dithioerythritol was performed on 10−15% gradient gels using the Phast^R System (Pharmacia, Uppsala, Sweden). Apparent molecular masses were determined from reduced gels, by comparison with a protein calibration mixture consisting of phosphorylase *b* (94 kDa), BSA (67 kDa), ovalbumin (45 kDa), carbonic anhydrase (30 kDa), soybean trypsin inhibitor (20.1 kDa), and α-lactalbumin (14.4 kDa). Densitometric scanning of SDS−PAGE was performed with the Gel-Scan Accessory of the Beckman DU60 spectrophotometer. Immunoblotting of nonreduced SDS−PAGE was performed according to Towbin (*19*), and autoradiography using the hypercasette from Amersham Life Science.

Protein concentrations were determined with the BCA (bicinchoninic acid) assay (Pierce Chemical Co.).

The 24k-endopeptidase (final concentration 80 μM) was digested with trypsin (10% mol/mol) overnight at 37 °C, and tryptic peptides were separated by HPLC using a Symmetry C18 column run with a gradient of 0−40% acetonitrile in 0.05% trifluoroacetic acid.

NH_2-terminal amino acid sequence analysis was performed on an Applied Biosystems model 477A protein sequencer (Foster City, CA), interfaced with an Applied Biosystems model 120A on-line analyzer. Samples were electrophoresed on 10−20% Tris-HCl Ready Gels (Mini-Protean^R II Cell; Bio-Rad, Hercules, CA), and blotted on ProBlott membranes (Applied Biosystems). Sequence analysis was performed with software (*20*) from the University of Wisconsin Genetics Computer Group, provided by the Belgian EMBL mode (Brussels, Belgium). Amino acid compositions were determined using the Pico.tag amino acid analysis system (Waters Corp., Milford, MA).

Table 1: Primers Used for Sequencing of 16S rDNA

	sequence (5′→3′)	position[a]
forward	CTC CTA CGG GAG GCA GCA GT	339−358
	CAG CAG CCG CGG TAA TAC	519−536
	AAC TCA AAG GAA TTG ACG G	908−926
	AGT CCC GCA ACG AGC GCA AC	1093−1112
	GCT ACA CAC GTG CTA CAA TG	1222−1241
reverse	ACT GCT GCC TCC CGT AGG AG	358−339
	GTA TTA CCG CGG CTG CTG	536−519
	GTT GCG CTC GTT GCG GGA CT	1112−1093

[a] Hybridizing position referring to the *E. coli* 16S rRNA gene sequence numbering.

A coupled chromogenic substrate assay was used to monitor proteolytic activity in bacterial culture medium and during purification; samples were added to a mixture of human plasminogen (final concentration 0.25 μM) and S-2403 (final concentration 0.3 mM), and the amidolytic activity was monitored from the absorbance at 405 nm for up to 6 h.

Endotoxin levels were determined using the microplate method of the Limulus Amebocyte Lysate (LAL) test kit (Coatest Endotoxin; Chromogenix AB).

Identification of Bacterial Strains. Identification of the bacterial strain secreting the endopeptidase was performed by BCCM/LMG (Laboratory for Microbiology, University of Ghent, Belgium).

To determine the phylogenetic position, genomic DNA was prepared according to the protocol of Niemann et al. (*21*), and 16S rRNA genes were amplified by PCR using the forward primer 5′-CTG GCT CAG GAC/T GAA CGC TG-3′ (hybridizing positions 19−38 referring to the *E. coli* 16S rRNA gene sequence numbering) and the reverse primer 5′-AAG GAG GTG ATC CAG CCG CA-3′ (hybridizing positions 1541−1522). PCR-amplified 16S rDNAs were purified using the QIAquick PCR Purification Kit (Qiagen GmbH, Hilden, Germany). Complete sequencing was performed using an Applied Biosystems, Inc., 377 DNA sequencer according to the protocols of the manufacturer (Perkin-Elmer, Applied Biosystems Division, Foster City, CA) using the ABI PRISM Big Dye Terminator Cycle Sequencing Ready Reaction Kit (with AmpliTaq^R DNA Polymerase, Fs). Forward and reverse primers used to get an optimal overlap of sequences are shown in Table 1. Sequence assembly was performed using the AutoAssembler program (Perkin-Elmer). Phylogenetic analysis was done with the software package Gene Compar (Applied Maths, Kortrijk, Belgium) after including the consensus sequence in an alignment of small ribosomal subunit sequences collected from the international nucleotide sequence library EMBL. The alignment was pairwise calculated using an open gap penalty of 100% and a unit gap penalty of 0%. A similarity matrix was created by homology calculation with a gap penalty of 0% and after discarding unknown bases. In addition, genomic DNA was prepared as described elsewhere (*22*), and DNA:DNA hybridizations were performed at 34 °C essentially according to the method of Ezaki et al. (*23*).

Bacterial Culture and Purification of 24k-Endopeptidase. Bacto-nutrient agar dishes (Oxoid CM3, pH 7.4) were inoculated with bacterial isolates, obtained from different fish species, and incubated at 28 °C. After incubation for about 20 h, a single colony was inoculated in 25 mL of nutrient

broth (casein peptone 0.5 g/L, meat peptone 0.5 g/L, yeast extract 2 g/L, peptone 5 g/L, pH 7.4) and cultured overnight at 25 °C, stirring at 120 rpm. This preculture was used to inoculate 2 L of the same nutrient broth, and fermented for 13 h at 28 °C with gentle stirring (100 rpm). Bacterial growth was continued to an optical density at 600 nm of 0.56 ± 0.03. After addition of 2 mL of a 10% (w/v) solution of flocculation polymers (Cat. floc-cl; Calgon), the culture broth was cooled to about 5 °C, and cells were removed by centrifugation for 10 min at 5000 rpm and 1 °C. The medium was sterile-filtered on a 0.22 μm cellulose acetate filter and frozen at −20 °C.

Purification was performed by a combination of hydrophobic interaction chromatography on Phenyl-Sepharose and ion exchange chromatography on SP−Sepharose (cf. Results).

Interaction with Substrates and Inhibitors. Different potential protein substrates (final concentration 3 μM) in 50 mM phosphate buffer, pH 7.4, containing 0.01% Tween 80, were incubated with the 24k-endopeptidase (final concentration 250 nM) for 1 h at 37 °C; samples were immediately heated at 100 °C for 3 min in 1% SDS, and the structure of the substrate was analyzed by SDS−PAGE under reducing and nonreducing conditions. Alternatively, 24k-endopeptidase (final concentration 400 nM) was preincubated for 10 min at 37 °C with different inhibitors prior to its addition to human plasminogen (final concentration 5 μM).

Effect on Cell-Associated Plasminogen Activation. Human THP-1 cells were washed 3 times with 50 mM HEPES buffer, pH 7.4, containing 0.01 M $CaCl_2$, 1.6 mM $MgSO_4$, 1% BSA, and 0.02% lactalbumin hydrolysate, and resuspended in this buffer at a density of 4×10^6 cells/mL. Incubation with human plasminogen (final concentration 100 nM) was performed in the presence of aprotinin (final concentration 20 KIU/mL) for 4 h at 4 °C, and unbound plasminogen was removed by centrifugation through 15% sucrose. The cells were again resuspended at a density of 4×10^6/mL in HEPES buffer, pH 7.4, containing 1% BSA, 0.02% lactalbumin hydrolysate, 20 KIU/mL aprotinin, and 300 μM amiloride, and incubated overnight at 37 °C with 24k-endopeptidase (final concentration 0−5 nM) in an incubator under 5% CO_2 and 95% humidity. The cells were recovered by centrifugation over 15% sucrose, and cell-associated plasminogen (6×10^5 cells/mL) was activated by addition of tcu-PA (final concentration 5 nM). Plasmin generation was monitored by addition of S-2403 (final concentration 0.3 mM) and measuring the change in absorbance at 405 nm. Blank samples without addition of tcu-PA but with 300 μM amiloride were used for background correction.

In separate experiments, ^{125}I-labeled plasminogen (final concentration 3 nM) was added to the plasminogen used for binding to the cells. At the end of the experiments, cell-bound plasminogen moieties were eluted with ϵ-ACA (final concentration 0.2 M) and subjected to SDS−PAGE followed by autoradiography or immunoblotting with monoclonal antibodies against plasminogen fragments.

Effects on Plasma Plasminogen. Human plasma or serum was incubated with the 24k-endopeptidase (final concentration 100 or 500 nM) for 1 h at 37 °C, followed by addition of lysine-Sepharose (100 μL suspension per milliliter) for 1 h at 37 °C. The gel was washed with 0.1 M phosphate buffer, pH 7.4, containing 0.01% Tween 80 and eluted with 50 mM ϵ-ACA in the same buffer. The eluates were applied to SDS−PAGE. Plasminogen activity levels in human plasma were measured with S-2403 after addition of excess streptokinase (*24*).

Purification and Functional Characterization of Plasminogen Fragments. Human plasminogen (final concentration 10 μM) was incubated with 24k-endopeptidase (final concentration 0.5 μM) for 2 h at 37 °C, as described above. The reaction mixture was applied to lysine-Sepharose equilibrated with 0.05 M phosphate buffer, pH 7.4, containing 0.01% Tween 80, and eluted with 50 mM ϵ-ACA (ϵ-aminocaproic acid). The break-through contains the miniplasminogen fragment, and the eluate containing the K1−4 fragment(s) and residual intact plasminogen was applied to Mab-42B12−Sepharose. The purified K1−4 fragments are recovered in the break-through, and intact plasminogen is eluted from the column with 0.1 M glycine, pH 2.8.

Cytotoxicity was evaluated with the ethidium homodimer-1 incorporation assay using bovine adrenal cortex-derived microvascular endothelial (BME) cells, as described elsewhere (*25*). Before the assay, endotoxin was removed from the K1−4 fragment by treatment with Remtox (Immunosource, Zoersel-Halle, Belgium), resulting in a decrease from 30 ng/mg of protein to <2 ng/mg, as measured with the LAL assay.

Kinetic analysis of the activation of miniplasminogen (final concentration 2.0−16 μM) by tcu-PA (final concentration 1.0 nM) at 37 °C in 0.1 M sodium phosphate buffer, pH 7.4, was performed by monitoring generated plasmin activity with S-2403 (final concentration 0.3 mM) for 4 min. Miniplasmin was prepared by activation of miniplasminogen with insolubilized tcu-PA. Kinetic constants of miniplasmin (final concentration 2 nM) for the hydrolysis of S-2403 (final concentration 0.05−1.0 mM) were determined by Lineweaver−Burk analysis following measurement of the change in absorbance at 405 nm at 37 °C in 0.1 M Tris-HCl buffer, pH 7.4, containing 0.038 M NaCl and 0.01% Tween 80 during 4 min (*26*).

RESULTS

Identification of Bacterial Strains. Culture medium of only 2 out of about 200 bacterial strains obtained from different fish species showed detectable activity in the coupled chromogenix substrate assay in the presence but not in the absence of plasminogen. The lowest activity was detected with an *Aeromones Sp.* culture and was not further characterized. The bacterial culture with the highest proteolytic activity showed a homogeneous growth on Tryptone Soya Agar medium at 28 °C, indicating its purity. Basic microbiological tests revealed a Gram-negative strain with positive oxidase and catalase reactions. Morphologically, cells appeared as rods ($0.9 \times 1.5-5$ μm), single or in pairs, nonmotile or without spores.

The consensus sequence of 16S rDNA, determined as described above, is shown in Figure 1. High sequence similarities with reference taxa of the genus *Chryseobacterium* were observed, indicating that the isolate phenotypically belongs to this genus. A sequence homology of ≥98% was observed with the species *Chryseobacterium indologenes* and *Chryseobacterium gleum*. DNA:DNA hybridizations re-

```
1     GCGGGAGGCCTAACACATGCAAGCCGAGCGGTAkAGATCTTTCGGGATCTTGAGAGCGGCGTAC
65    GGGTGCGGAACACGTGTGCAACCTGCCTTTATCAGGGGGATAGCCTTTCGAAAGGAAGATTAAT
129   ACCCCATAATATTTAGAATGGCATCATTTTAAATTGAAAACTCCGGTGGATAGAGATGGGCACG
193   CGCAAGATTAGATAGTTGGTGAGGTAACGGCTCACCAAGTCAGCGATCTTTAGGGGGCCTGAGA
257   GGGTGATCCCCCACACTGGTACTGAGACACGGACCAGACTCCTACGGGAGGCAGCAGTGAGGAA
321   TATTGGACAATGGGTGCGAGCCTGATCCAGCCATCCCGCGTGAAGGACGACGGCCCTATGGGTT
385   GTAAACTTCTTTTGTATAGGGATAAACCCAGATACGTGTATCTGGCTGAAGGTACTATACGAAT
449   AAGCACCGGCTAACTCCGTGCCAGCAGCCGCGGTAATACGGAGGGTGCAAGCGTTATCCGGATT
513   TATTGGGTTTAAAGGGTCCGTAGGCTGATTTGTAAGTCAGTGGTGAAATCTCACAGCTTAACTG
577   TGAAACTGCCATTGATACTGCAAGTCTTGAGTGTTGTTGAAGTAGCTGGAATAAGTAGTGTAGC
641   GGTGAAATGCATAGATATTACTTAGAACACCCATTGCGAAGGCAGGTTACTAAGCAACAACTGA
705   CGCTGATGGACGAAAGCGTGGGGAGCGAACAGGATTAGATACCCTGGTAGTCCACGCCGTAAAC
769   GATGCTAACTCGTTTTTGGGTTTTCGGATTCAGAGACTAAGCGAAAGTGATAAGTTAGCCACCT
833   GGGGAGTACGAACGCAAGTTTGAAACTCAAAGGAATTGACGGGGGCCCGCACAAGCGGTGGATT
897   ATGTGGTTTAATTCGATGATACGCGAGGAACCTTACCAAGGCTTAAATGGGAAATGACAGGTTT
961   AGAAATAGACTTTTCTTCGGACATTTTTCAAGGTGCTGCATGGTTGTCGTCAGCTCGTGCCGTG
1025  AGGTGTTAGGTTAAGTCCTGCaACGAGCGCAACCccTGTCAcTAGTTGCCATCATTAAGTTGGG
1089  GACTCTAGTGAGACTGCCTACGCAAGTAGAGAGGAAGGTGGGGATGACGTCAAATCATCACGGC
1153  CcTTACGccTTGGGCCACAcACGTAATACAATGGCCGGTACAGAGGGCAGCTACACAGTGATGT
1217  GATGCAAATCTCGAAAGCCGGTCTCAGTTCGGATTGGAGTCTGCAACTCGACTCTATGAAGCTG
1281  GAATCGCTAGTAATCGCGCATCAGCCATGGCGCGGTGAATACGTTCCCGGGCCTTGTACACACC
1345  GCCCGTCAAGCCATGGAAGTCTGGGGTACCTGAAGTCGGTGACCGTAACAGGAGCTGCCTAGGG
1409  TAAAACAGGTAACTAGGGCTAAGTCGTAACAAGGTAGCCGTACCGGAAGG
```

FIGURE 1: Consensus sequence of 16S rDNA isolated from *Chryseobacterium Sp*.

vealed, however, only 33% or 44% DNA homology with *C. indologenes* or *C. gleum*, indicating that a new species in the genus *Chryseobacterium* was isolated.

Purification and Physicochemical Characterization. Culture medium (5 L batches) with addition of 0.5 M NaCl was applied to a 1.6 × 13 cm column of Phenyl-Sepharose equilibrated with 10 mM phosphate buffer, pH 6.0, containing 0.5 M NaCl, at 4 °C and a flow rate of 300−400 mL/h. The column was washed with 10 mM phosphate buffer, pH 6.0, containing 1 M NaCl, and eluted with 40% ethylene glycol. Under these conditions, only about 0.02% of the total protein was recovered in the eluate, whereas the supernatant was virtually devoid of activity as monitored with the coupled chromogenic substrate assay. After desalting on Sephadex G-25 in 10 mM phosphate buffer, pH 6.0, the sample (70 mL with $A_{1cm}^{280nm} = 0.05$) was applied to a 1 × 2 cm column of SP−Sepharose equilibrated with the same buffer at 4 °C and a flow rate of 120 mL/h. The column was eluted with a linear gradient of the equilibration buffer to 1 M NaCl in the same buffer; the activity eluted at 0.3 M NaCl. The final yields of two subsequent preparations were 420 and 330 μg/L of medium, and the purified protein represented about 0.008% of the total protein in the culture medium at the start. The protein was homogeneous and consisted of a single polypeptide chain of 24 kDa as shown by SDS−PAGE (Figure 2, lanes 3). NH_2-terminal amino acid sequence analysis revealed a major homogeneous sequence (>90% yield) corresponding to Val-Ala-Thr-Pro-Asn-Leu-Glu-Ser-Val-Gln-Thr-Tyr-Leu-Asn-Asp-. Sequencing of a purified tryptic peptide yielded the sequence Tyr-Arg-Pro-Asn-Glu-Leu-Glu-Ala-. No sequence presenting significant similarity to these sequences could be identified with BLAST (Gapped BLAST and PSI-BLAST) (*27*) and FASTA (*20*) searches in the SwissProt databank, or on translation of the whole GenBank/EMBL Nucleotide Sequence Database.

Amino acid analysis revealed that the protein consists of the following amino acids (% of total residues; mean ± SEM, $n = 4$): Asp (11.5 ± 1.0%), Glu (7.3 ± 0.53%), Ser (5.1 ± 0.52%), Gly (10.9 ± 0.12%), His (1.3 ± 0.08%), Arg (4.9 ± 0.44%), Thr (4.2 ± 0.47%), Ala (9.4 ± 0.07%), Pro (5.1 ± 0.18%), Tyr (13.1 ± 0.54%), Val (4.4 ± 0.16%), Met (0.72 ± 0.07%), Ile (5.4 ± 0.15%), Leu (8.6 ± 0.07%), Phe (6.1 ± 0.44%), and Lys (2.2 ± 0.11%).

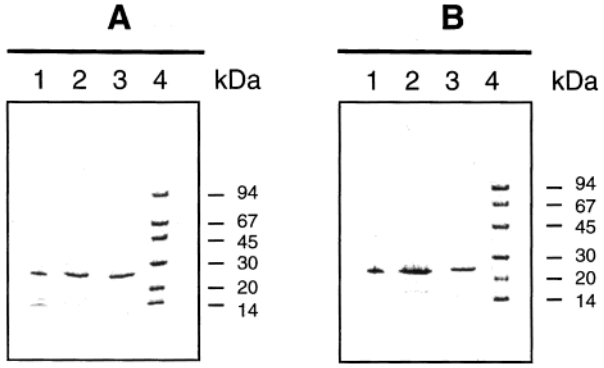

FIGURE 2: Purification of 24k-endopeptidase from conditioned culture medium of *Chryseobacterium Sp.* Three microliter samples (with A_{1cm}^{280nm} adjusted to 0.3) were applied to SDS−PAGE using 10−15% gradient gels under nonreducing (A) or reducing (B) conditions. Lane 1, eluate from Phenyl-Sepharose; lane 2, sample after desalting on Sephadex G-25; lane 3, eluate from SP−Sepharose; lane 4, protein calibration mixture.

Interaction with Substrates and Inhibitors. Incubation of human, murine, rabbit, baboon, canine, or bovine plasminogen with 24k-endopeptidase at an E/S ratio of 1/12 for 1 h at 37 °C revealed nearly complete degradation of human plasminogen (<1% residual plasminogen as determined by densitometric scanning of reduced SDS−PAGE) and of baboon plasminogen (6% residual protein), whereas canine (51% residual protein), bovine (57% residual protein), rabbit (69% residual protein), and murine (88% residual protein) plasminogens appeared more resistant to proteolysis. Incubation with other macromolecular substrates under the same experimental conditions, followed by SDS−PAGE under reducing conditions, did not reveal significant hydrolysis of human α_2-antiplasmin, albumin, or IgG.

At a final concentration of 1 μM 24k-endopeptidase in 0.05 M Tris-HCl buffer, pH 7.4, containing 0.038 M NaCl and 0.01% Tween 80 at 37 °C, no hydrolysis was observed of the following chromogenic substrates (final concentration

1 mM) as monitored from the absorbance at 405 nm: S-2251 (H-D-Val-Leu-Lys-pNA), S-2403 (pyroGlu-Phe-Lys-pNA), S-2518 (Ser-Pro-Pro-pNA), S-2495 (Thr-Pro-Pro-pNA), S-2533 (Ser-Thr-Pro-Pro-pNA), S-2526 (Bz-Ser-Pro-Pro-pNA), or S-2524 (Bz-Thr-Pro-Pro-pNA).

The capacity of 24k-endopeptidase to cleave plasminogen was not significantly affected by preincubation (at a final concentration of 400 nM) for 10 min at 37 °C with the following inhibitors (molar excess indicated in parentheses): α_2-antiplasmin (8 ×), aprotinin (8 ×), NPGB (8000 ×), TPCK (40 000 ×), PMSF (40 000 ×), leupeptin (600 ×), pepstatin (400 ×), or EDTA (100 000 ×). At 4000−40 000-fold molar excess of 1,10-phenanthroline, some inhibition became apparent (about 50% residual plasminogen); the cleavage pattern was similar to that normally obtained in the initial stage of the reaction (Figure 4A, lane 2).

Incubation of 24k-endopeptidase with 3−5-fold molar excess of α_2-macroglobulin, however, resulted in formation of a complex migrating with an apparent M_r of 180 000 on reduced SDS−PAGE (not shown). Furthermore, a mixture of 24k-endopeptidase (final concentration 100 nM) and α_2-macroglobulin (at 5-fold molar excess) showed a significantly impaired capacity to hydrolyze plasminogen (final concentration 2 μM) in a buffer milieu, as compared to the enzyme alone under identical experimental conditions. Densitometric scanning of nonreduced SDS−PAGE revealed 100%, 91%, and 66% residual plasminogen after incubation with the mixture for 5, 20, and 30 min, at 37 °C, whereas with the enzyme alone residual plasminogen was 6.9%, 2.1%, and 12% at the same time points.

Characterization of the Interaction with Plasmin(ogen). Incubation of human plasminogen (final concentration 5 μM) with 24k-endopeptidase (final concentration 400 nM) in 50 mM phosphate buffer, pH 7.4, containing 0.01% Tween 80 for 1 h at 37 °C, yielded ≤2% plasmin-like activity as determined with S-2403 (final concentration 0.3 mM).

This suggests that the plasmin-like activity initially detected in the culture medium with the plasminogen-coupled chromogenic substrate assay is not generated by a true plasminogen activator, but may arise from some amidolytic activity in the mixture of plasmin(ogen) and cleavage products with the endopeptidase.

Addition of CNBr-digested fibrinogen (final concentration 0.5 μM) to the incubation mixture did not affect the activation rate of plasminogen. Under the same experimental conditions, tcu-PA (final concentration 50 nM) induced about 90% plasminogen activation within 3−4 min (not shown).

SDS−PAGE of the reaction mixtures revealed that native plasminogen was quantitatively converted to four lower M_r fragments. Addition of human α_2-antiplasmin (final concentration 100 nM), at the end of the incubation, did not yield detectable amounts of complexes with plasmin-like moieties as revealed by SDS−PAGE under nonreducing conditions (not shown), confirming the absence of plasmin activity.

To study the interaction of 24k-endopeptidase with plasminogen in more detail, the time course of proteolysis was analyzed using different enzyme/substrate ratios (1/60−1/6). As shown in Figure 3, limited digestion was obtained within 10 min at E/S ratios of 1/60 and 1/30, whereas ≥80% digestion was achieved at E/S ratios of 1/12 and 1/6. SDS−PAGE showed a complex degradation pattern, with three

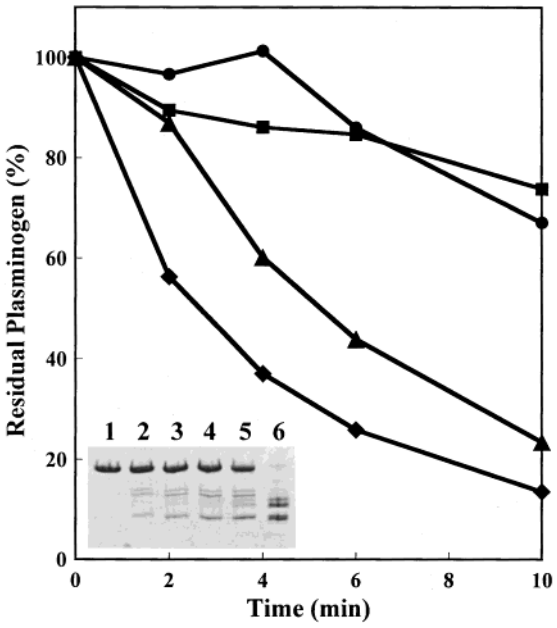

FIGURE 3: Time course of proteolytic cleavage of plasminogen by 24k-endopeptidase, at enzyme/substrate ratios of 1/60 (■), 1/30 (●), 1/12 (▲), or 1/6 (◆). The area corresponding to residual intact plasminogen at different time points was determined by densitometric scanning of nonreduced SDS−PAGE and expressed as percent of the amount present at the start. The inset shows the time course obtained at 1/60 enzyme/substrate ratio, with lane 1 corresponding to the start, and lanes 2−5 to 2, 4, 6, and 10 min, respectively. Lane 6 shows the degradation pattern at 1/6 enzyme/substrate ratio after 10 min.

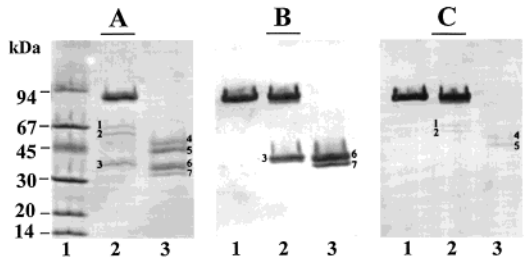

FIGURE 4: SDS−PAGE under nonreducing conditions (panel A) after incubation of plasminogen with 24k-endopeptidase for 4 min at E/S of 1/60 (lane 2), or for 1 h at E/S of 1/12 (lane 3). Lane 1 represents the protein calibration mixture. Panels B and C show immunoblotting of the samples in panel A with MAb-42B12 and MAb-36E6, respectively.

bands appearing very rapidly (Figure 3, inset, lanes 2−4); subsequently the two upper bands convert into two lower M_r bands, and the lower band converts into a doublet (Figure 3, inset, lanes 5 and 6).

To further characterize the molecular structure of the generated plasminogen fragments, digestion was performed under conditions yielding the three early products (E/S of 1/60 for 4 min; Figure 4A, lane 2) or yielding the four late products (E/S of 1/12 for 1 h; Figure 4A, lane 3). NH_2-terminal amino acid sequence analysis of the different plasminogen moieties identified several cleavage sites in the plasminogen molecule (Table 2 and Figure 5). The sequence data are compatible with the following pattern: first, cleavage of the Ser^{441}−Val^{442} peptide bond, yielding fragments 1 and 2 (cf. Figure 4) (corresponding to the NH_2-terminal fragment comprising Glu^1−Ser^{441}, possibly with some COOH-terminal or carbohydrate heterogeneity) and fragment 3 (correspond-

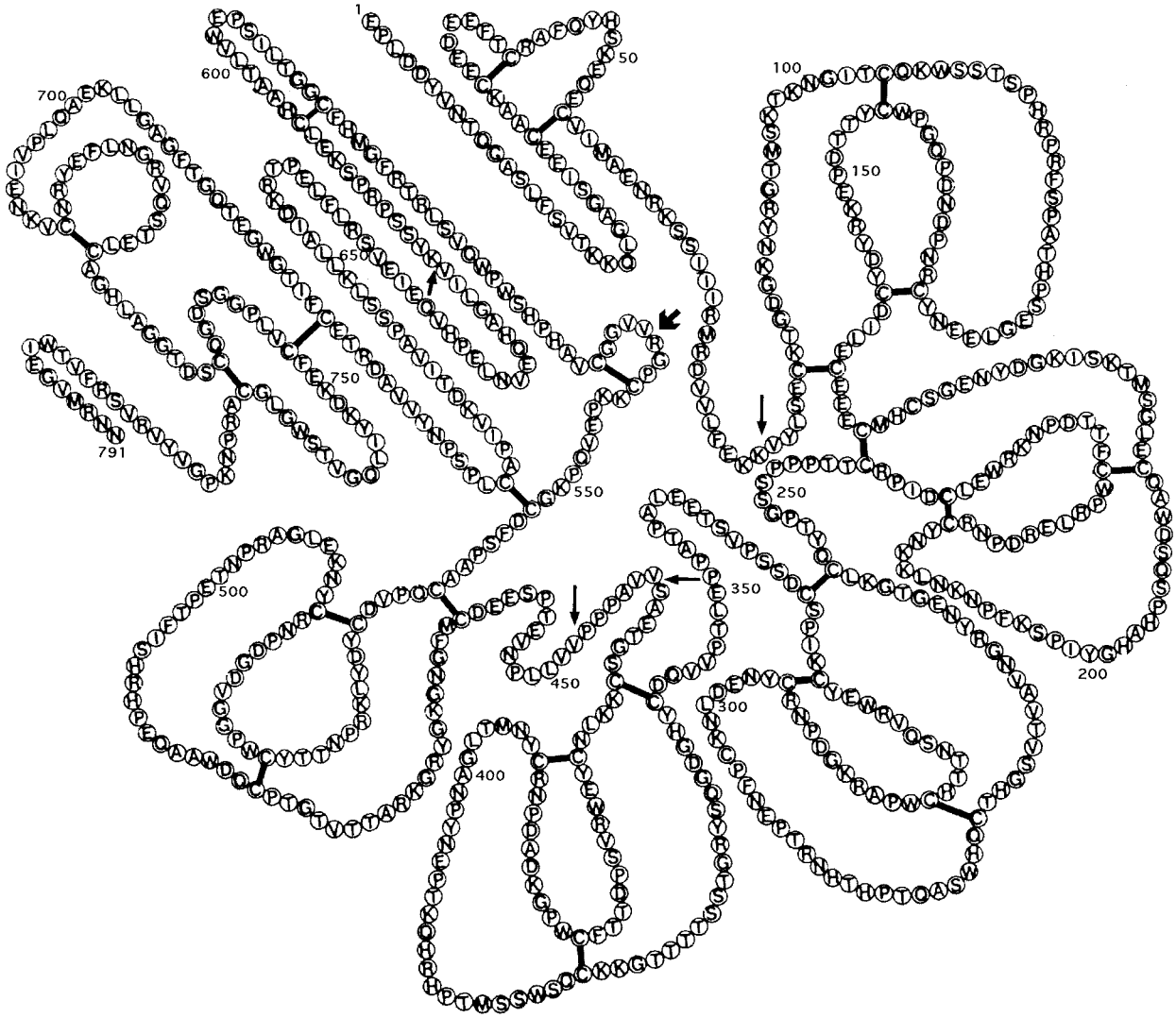

FIGURE 5: Schematic representation of the primary structure of human plasminogen. The amino acids are represented by their single-letter symbols, and black bars indicate disulfide bonds (adopted from refs *5* and *6*). An additional disulfide bond between Cys^{169} and Cys^{297} is not represented. The arrows indicate the cleavage sites of 24k-endopeptidase (→) and of plasminogen activators (➞).

Table 2: NH_2-Terminal Amino Acid Sequence Analysis of Plasminogen Treated with 24k-Endopeptidase (Enzyme/Substrate Ratio of 1/100 for 4 min at 37 °C for Fragments 1−3 and 1/20 for 1 h at 37 °C for Fragments 4−7)

	amino acid (recovery in pmol) in cycle						
fragment[a]	1	2	3	4	5	6	7
1	Glu (10)	Pro (9)	Leu (7)	Asp (5)	Asp (9)	Tyr (5)	Val (7)
2	Glu (19)	Pro (16)	Leu (11)	Asp (7)	Asp (12)	Tyr (8)	Val (10)
3	Val (20)	Val (17)	Ala (13)	Pro (15)	Pro (19)	Pro (14)	Val (10)
4	Val (63)	Tyr (40)	Leu (40)	Ser (15)	Glu (18)	Cys (−)	Lys (17)
5	Val (91)	Tyr (65)	Leu (66)	Ser (13)	Glu (26)	Cys (−)	Lys (23)
6	Val (178)	Ile (57)	Leu (128)	Gly (71)	Ala (49)	His (22)	Gln (27)
	Val (178)	Val (99)	Leu (128)	Leu (78)	Pro (68)	Asx (63)	Val (55)
7	Val (75)	Val (65)	Leu (41)	Leu (42)	Pro (34)	Asx (17)	Val (26)

[a] Fragments as shown in Figure 4A.

ing to the COOH-terminal region comprising Val^{442}−Asn^{791}). These structures are compatible with the molecular weights of the fragments, and are further confirmed by immunoblotting with MAb-42B12 (Figure 4B, lane 2), indicating the presence of kringle 5 in fragment 3, and with MAb- 36E6 (Figure 4C, lane 2), indicating the presence of kringles 1−3 in fragments 1 and 2. Additional cleavages involve the Lys^{78}−Val^{79} peptide bond, converting fragments 1 and 2 into fragments 4 and 5 (both representing an NH_2-terminal fragment starting with Val^{79}), and the Pro^{447}−Val^{448} peptide bond, converting fragment 3 into fragments 6 and 7 (both respresenting a COOH-terminal fragment starting with Val^{448}). Fragment 6 contains a second sequence, starting at Val^{616} (cleavage of Lys^{615}−Val^{616}), and thus consists of two disulfide-bonded fragments (Val^{448} to Lys^{615} and Val^{616} to Asn^{791}). This is compatible with the observation that upon SDS−PAGE under reducing conditions band 6 disappears as a result of reduction of the Cys^{548}−Cys^{566} disulfide bond (not shown). The structures of these late degradation products are again compatible with their molecular weights, and are further confirmed by immunoblotting with MAb-42B12 (Figure 4B, lane 3), indicating the presence of kringle 5 in fragments 6 and 7, and with MAb-36E6 (Figure 4C, lane 3), indicating the presence of kringles 1−3 in fragments 4 and 5.

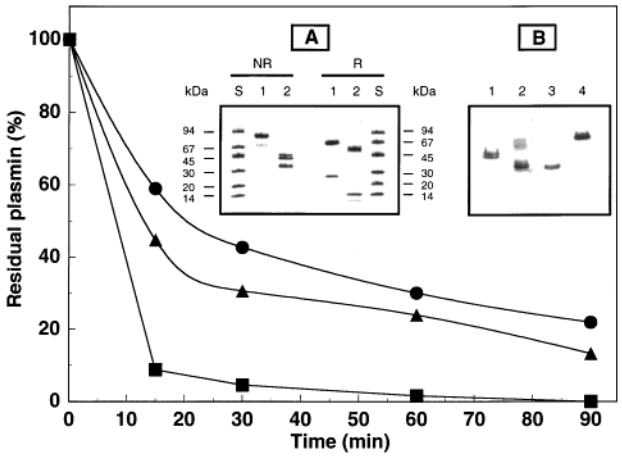

FIGURE 6: Time course of proteolytic cleavage of plasmin by 24k-endopeptidase, at E/S ratio of 1/12. At different time points, residual plasmin-like activity was determined with S-2403 (●), residual intact plasmin (■) by densitometric scanning of nonreduced SDS−PAGE, and residual plasmin B-chain (▲) from reduced SDS−PAGE; the data are expressed as percent of the amount present at the start. Inset A shows SDS−PAGE under nonreducing (NR) or reducing (R) conditions of samples taken at time 0 (lanes 1) or after 90 min reaction (lanes 2). Lanes S represent the protein calibration mixture. Inset B shows immunoblotting (nonreduced) of the 90 min sample with MAb-36E6 (lane 1), MAb-42B12 (lane 2), or MAb-31E9 (lane 3) and of intact plasmin with MAb-31E9 (lane 4).

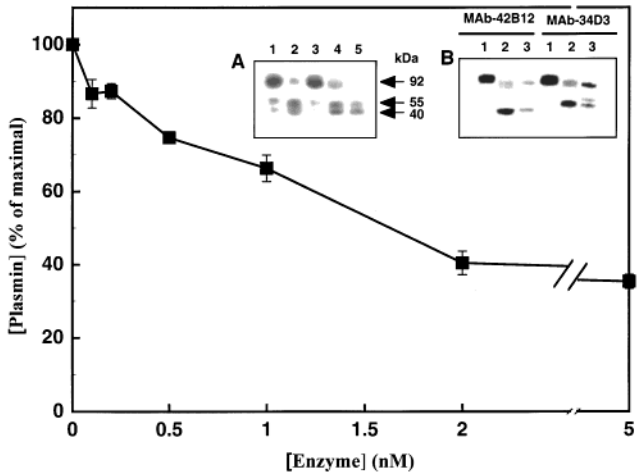

FIGURE 7: Effect of 24k-endopeptidase on plasminogen bound to THP-1 cells. The concentration of cell-associated plasmin after activation with tcu-PA (expressed in % of that obtained without 24k-endopeptidase) is plotted versus the concentration used. The data represent mean ± SEM of 3 independent experiments. Inset A shows autoradiographs, representing purified ^{125}I-plasminogen before (lane 1) or after treatment with 24k-endopeptidase (lane 2), the plasminogen eluted from THP-1 cells without (lane 3) or with treatment (lane 4), and the supernatant after treatment (lane 5). Inset B shows immunoblotting of purified plasminogen without (lanes 1) or after treatment (lanes 2), and of the eluate of THP-1 cells treated with 24k-endopeptidase (lanes 3), using MAb-34D3 or MAb-42B12.

Incubation of human plasmin (final concentration 3 μM) with 24k-endopeptidase (final concentration 250 nM) also resulted in rapid time-dependent proteolysis as shown by densitometric scanning of SDS−PAGE under nonreducing and reducing conditions (Figure 6). The NH_2-terminal fragments (upper two bands in Figure 6, inset A, lane 2, NR) have comparable M_r as those obtained from plasminogen (bands 4 and 5 in Figure 4A, lane 3), whereas the COOH-terminal fragments have comparable M_r on nonreduced SDS−PAGE, but show dissociation of kringle 5 upon reduction and degradation of the B-chain (Figure 6, inset A). The amidolytic activity, as measured with S-2403, decreased somewhat more slowly than expected from the disappearance rate of the protein. This is most likely due to the fact that, after initial cleavage at Ser^{441} or Pro^{447}, the isolated B-chain still retains some activity, as suggested by the similar time-dependent disappearance of the B-chain (protein) and of the amidolytic activity. Subsequent inactivation of the plasmin B-chain probably occurred due to cleavage of the Lys^{615}−Val^{616} peptide bond and further degradation. Immunoblotting (90 min samples) with MAb-36E6 (Figure 6, inset B, lane 1) confirmed that the upper two bands contain kringles 1−3, whereas the lower band consists of mini-plasmin, as shown by its immunoreactivity with MAb-42B12 (Figure 6, inset B, lane 2) and with MAb-31E9 (Figure 6, inset B, lane 3).

Effect on Cell-Associated Plasminogen Activation. Under the experimental conditions used, the viability of THP-1 cells was >95%, and binding of plasminogen (as determined in separate experiments with ^{125}I-plasminogen) amounted to about 15−20 nM, corresponding to (2.7 ± 0.6) × 10^6 molecules bound per cell (mean ± SEM, n = 3).

As shown in Figure 7, incubation of cell-associated plasminogen with 24k-endopeptidase (final concentration 0−5 nM) resulted in a dose-dependent reduction of the concentration of cell-bound plasmin that could be generated upon activation with tcu-PA. Autoradiography showed the presence of intact plasminogen in eluates of cells not treated with 24k-endopeptidase (Figure 7, inset A, lane 3), while after treatment two plasminogen moieties of about 55 and 40 kDa were observed in the eluate and in the supernatant (Figure 7, inset A, lanes 4 and 5). Immunoblotting with monoclonal antibodies revealed that the 55 kDa band corresponds to the NH_2-terminal region of plasminogen containing the kringles (recognized by MAb-34D3), and the 40 kDa band to miniplasmin (recognized by MAb-42B12) (Figure 7, inset B, lanes 3).

Effect on Plasma Plasminogen. Incubation of human plasma or serum (containing >90% residual plasminogen) with 24k-endopeptidase (enzyme/substrate ratio of 1/20 or 1/4) for 1 h at 37 °C resulted in only minor plasminogen degradation, as shown by SDS−PAGE after adsorption with lysine-Sepharose. The pattern was similar to that seen upon early digestion of plasminogen in a buffer milieu (cf. Figure 4A, lane 2, bands 1 and 2), showing mainly intact plasminogen and a small amount of lysine-binding site containing fragments eluted from lysine-Sepharose. Essentially the same result was obtained after incubation with 100 nM 24k-endopeptidase for 24 h (not shown). Measurement of residual plasminogen activity in human plasma following incubation with 24k-endopeptidase (final concentration 50−200 nM) for up to 19 h at 37 °C did not reveal loss of plasminogen activity (not shown).

Purification and Functional Characterization of Plasminogen Fragments. Chromatography of plasminogen digested with 24k-endopeptidase on lysine-Sepharose yielded purified miniplasminogen in the break-through (Figure 8A, lane 3). Upon reduction (Figure 8B, lane 3), the miniplasminogen was separated into two fragments, probably as a result of

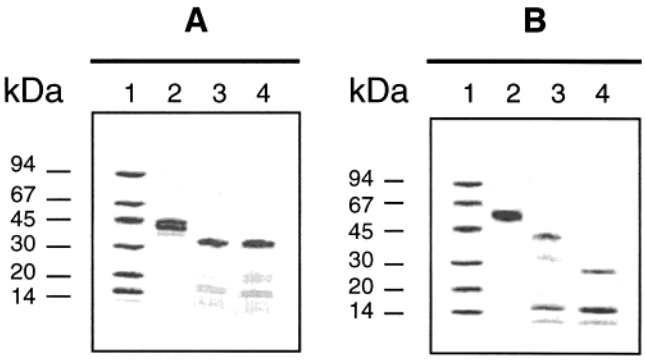

FIGURE 8: SDS-PAGE under nonreducing (panel A) or reducing (panel B) conditions of the purified K1−4 plasminogen fragment (lanes 2), and of purified miniplasminogen generated with 24k-endopeptidase (lanes 3), and of the corresponding miniplasmin derivative (lanes 4). Lanes 1 show the protein calibration mixture.

cleavage of the Lys^{615}−Val^{616} peptide bond and/or additional degradation. Chromatography of the eluate on MAb-42B12−Sepharose yielded purified K1−4 fragment(s) in the breakthrough (Figure 8A,B, lanes 2). The final yields of the purified K1−4 and miniplasminogen fragments were about 5 mg starting from 10 mg of native plasminogen, representing nearly quantitative recovery.

The endogeneous amidolytic activity against S-2403 of the purified miniplasminogen corresponded to a plasmin activity of <0.02%. Activation with tcu-PA obeyed Michaelis−Menten kinetics as evidenced by linear double-reciprocal plots of the initial activation rates versus the substrate concentration (not shown). K_m and k_{cat} values determined by linear regression analysis were 16 μM and 2.1 s^{-1} (r = 0.99), as compared to K_m = 8 μM and k_{cat} = 3.8 s^{-1} (r = 0.99) for elastase-derived miniplasminogen. SDS−PAGE under reducing conditions showed conversion of the miniplasmin moiety into a 14 kDa fragment (the K5 domain), whereas only part of the B-chain remained intact (Figure 8B, lane 4).

Activation with insolubilized tcu-PA resulted in conversion of 20% or 60% of 24k-endopeptidase- or elastase-derived miniplasminogen into plasmin-like activity (as monitored with 0.3 mM S-2403, using a conversion factor of 30 mA_{405nm}/min for 1 nM activity). The lower yield with the 24k-endopeptidase-derived moiety is probably due to further degradation of the plasmin B-chain, as also shown in Figure 6. The kinetic parameters of the generated miniplasmin for hydrolysis of S-2403 (K_m = 0.07 mM and k_{cat} = 73 s^{-1}; r = 0.99) were similar to those of the elastase-derived moiety (K_m = 0.08 mM and k_{cat} = 71 s^{-1}; r = 0.99).

Cytotoxic effects were monitored by treatment of BME cells for 48 h with different concentrations of plasminogen, K1−4, or elastase-derived K1−3 (Technoclone, Vienna), followed by quantitation of the percentage of dying cells using the ethidium homodimer incorporation assay. With the K1−4 fragment, very low cytotoxicity was observed at doses from 1 to 100 ng/mL (≤3%) whereas at doses of 1 or 10 μg/mL 5% or 12.7% (mean of 2 independent experiments) of the cells incorporated the dye. Elastase-derived K1−3 at a dose of 10 μg/mL caused 10.6% cytotoxicity, whereas purified plasminogen did not induce detectable cytotoxicity at doses between 2.2 ng/mL and 22 μg/mL. At the highest concentration of the K1−4 fragment used, endotoxin levels were maximally 20 pg/mL, which is far below the lowest cytotoxic concentration of isolated endotoxin in this assay (1 μg/mL) (*25*).

DISCUSSION

A previously unknown 24 kDa endopeptidase has been purified from conditioned medium of a bacterial strain which was identified on the basis of its 16S rDNA sequence as belonging to the genus *Chryseobacterium.* The 16 S rDNA showed the highest sequence similarity with that of *Chryseobacterium indologenes* and *Chryseobacterium gleum.* DNA:DNA hybridization assays did, however, only reveal a low degree of homology, indicating that we have isolated a new species in the genus *Chryseobacterium.*

Treatment with inhibitors against enzymes of the serine, cysteine, aspartic, or matrix metalloproteinase classes only revealed partial inhibition of the 24k-endopeptidase by high concentrations of 1,10-phenanthroline. However, the observations that the activity was not inhibited by EDTA and was preserved in the absence of added metal ions argues against a typical metalloproteinase nature. In human plasma or serum, the enzymatic activity was impaired, apparently due to neutralization by α_2-macroglobulin.

The 24k-endopeptidase specifically hydrolyzes human plasminogen, thereby generating an angiostatin-like fragment, containing kringles 1−4, and decreasing cellular binding of plasminogen. This results in a reduced capacity to generate cell-associated plasmin activity. After cleavage, in addition to the kringle-containing fragment, some low M_r plasminogen also remained associated with the cells, as has been observed previously (*28*). Angiostatin has recently attracted great attention because of its antiangiogenic potential, and a recombinant form is presently under investigation as a therapeutic agent for treatment of cancer (*29*). Several mechanisms were reported for angiostatin generation. Thus, macrophage-derived metalloelastase may contribute to angiostatin generation in the murine Lewis lung carcinoma model (*30*). In human prostate carcinoma cells (PC-3), u-PA and free sulfhydryl donors are involved in angiostatin formation (*31*). It may also be generated by plasmin autodigestion in a reaction catalyzed by a protein disulfide isomerase or in the presence of a free sulfhydryl donor (*31, 32*). In addition, some matrix metalloproteinases can generate angiostatin: MMP-3 (stromelysin-1) cleaves the Glu^{59}−Asn^{60}, Pro^{447}−Val^{448}, and Pro^{544}−Ser^{545} peptide bonds in plasminogen (*33*); MMP-7 (matrilysin) and MMP-9 (gelatinase B) both hydrolyze the Lys^{77}−Lys^{78} peptide bond, and MMP-7 also cleaves the Pro^{447}−Val^{448} bond, whereas MMP-9 hydrolyzes Pro^{446}−Pro^{447} (*34*).

The 24k-endopeptidase of *Chryseobacterium Sp.* cleaves the Ser^{441}−Val^{442} peptide bond, followed by the Lys^{78}−Val^{79}, Pro^{447}−Val^{448}, and Lys^{615}−Val^{616} peptide bonds, thus generating an angiostatin-like fragment similar to that obtained with MMPs. The cytotoxicity of this fragment against endothelial cells is comparable to that of the elastase-derived K1−3 fragment of plasminogen. Similar data were obtained as reported previously with other angiostatin preparations (*25*). The potential contribution of protein-bound endotoxin to the observed cytotoxicity remains, however, to be studied in more detail.

All four peptide bonds in human plasminogen that are susceptible to cleavage by 24k-endopeptidase have Val in

the P'_1 position, and Lys, Ser, or Pro in the P_1 position. In baboon plasminogen, which is cleaved equally well as human plasminogen, all four peptide bounds are conserved, whereas in bovine plasminogen, which is only partially cleaved, Ser^{441} is substituted with Gln and $Pro^{447}-Val^{448}$ is deleted. In murine plasminogen, which is resistant to cleavage, Lys^{78} is substituted with Arg and Pro^{447} with Thr (*35*). Furthermore, peptide chromogenic substrates with Lys or Pro in the P_1 position are not cleaved at any detectable rate.

Several mechanisms may contribute to the invasive behavior of bacteria. Invasive bacteria can use cell-surface-associated plasmin to facilitate movement through normal tissue barriers. Many pathogenic bacteria indeed bind plasmin(ogen) as well as plasminogen activators, and plasmin generated at the cell surface is protected from inhibition by physiological proteinase inhibitors (*36*−*38*). Thus, an organism with plasmin bound to its surface may be able to escape from a fibrin network deposited by the host to contain a focus of infection. Several bacteria produce plasminogen activators, e.g., streptokinase and staphylokinase, and many bacterial proteinases not only are resistant to host plasma proteinase inhibitors (serpins) but also rapidly inactivate them (*39*). The interactions between bacteria and the host fibrinolytic system thus are complex and depend on the site of infection and the availability of plasmin(ogen), plasminogen activators, and inhibitors (*36*).

The interaction of the 24k-endopeptidase purified from *Chryseobacterium Sp.* with plasmin(ogen) appears, however, to have different effects. It indeed removes the kringle 1−4 domains which are involved in cellular receptor binding, resulting in reduced binding of plasmin(ogen). In addition, plasminogen bound to the cell surface is also cleaved, resulting in removal of the serine proteinase domain, and in a reduced capacity to generate cell-associated plasmin (as shown with THP-1 cells). In that respect, this proteinase thus could reduce bacterial invasion. Although this *Chryseobacterium Sp.* was obtained from fish, some closely related bacterial strains, e.g., *Flavobacterium meningosepticum*, can also infect humans. It is unclear, however, whether reduced cellular proteolytic activity or generation of an angiostatin-like fragment play any role in bacterial pathogenesis.

ACKNOWLEDGEMENT

Cytotoxicity assays were performed by courtesy of Dr. R. Lucas (Laboratory of Immunopathology, Geneva University Hospital, Switzerland) and Dr. M. S. Pepper (Department of Morphology, University Medical Center, Geneva, Switzerland). NH_2-terminal amino acid sequence analysis was performed by courtesy of Prof. F. Van Leuven (Center for Human Genetics, University of Leuven, Belgium), and amino acid compositions were determined by courtesy of Prof. W. Rombauts (Biochemistry, University of Leuven, Belgium). We are grateful to E. Demarsin for expert technical assistance with purifications.

REFERENCES

1. Collen, D., and Lijnen, H. R. (1991) *Blood 78*, 3114−3124.
2. Ploplis, V. A., Carmeliet, P., Vazirzadeh, S., Van Vlaenderen, I., Moons, L., Plow, E. F., and Collen, D. (1995) *Circulation 92*, 2585−2593.
3. Carmeliet, P., and Collen, D. (1998) *Thromb. Res. 91*, 255−285.
4. Plow, E. F., Ploplis, V. A., Carmeliet, P., and Collen, D. (1999) *Fibrinolysis Proteolysis 13*, 49−53.
5. Sottrup-Jensen, L., Petersen, T. E., and Magnusson, S. (1978) *Atlas of Protein Sequences*, p 91, National Biomedical Research Foundation, Washington, DC.
6. Forsgren, M., Raden, B., Israelsson, M., Larsson, K., and Heden, L. O. (1987) *FEBS Lett. 213*, 254−260.
7. Wallen, P., and Wiman, B. (1970) *Biochim. Biophys. Acta 221*, 20−30.
8. Wallen, P., and Wiman, B. (1972) *Biochim. Biophys. Acta 257*, 122−134.
9. Collen, D. (1980) *Thromb. Haemostasis 43*, 77−89.
10. Lijnen, H. R., Bachmann, F., Collen, D., Ellis, V., Pannekoek, H., Rijken, D. C., and Thorsen, S. (1994) *J. Intern. Med. 236*, 415−424.
11. O'Reilly, M. S., Holmgren, L., Shing, Y., Chen, C., Rosenthal, R. A., Moses, M., Lane, W. S., Cao, Y., Sage, E. H., and Folkman, J. (1994) *Cell 79*, 315−328.
12. Cao, Y., Ji, R. W., Davidson, D., Schaller, J., Marti, D., Söhndel, S., McCance, S. G., O'Reilly, M. S., Llinas, M., and Folkman, J. (1996) *J. Biol. Chem. 271*, 29461−29467.
13. Sim, B. K. L., O'Reilly, M. S., Liang, H., Fortier, A. H., He, W., Madsen, J. W., Lapcevich, R., and Nacy, C. A.(1997) *Cancer Res. 57*, 1329−1334.
14. Wu, Z., O'Reilly, M. S., Folkman, J., and Shing, Y. (1997) *Biochem. Biophys. Res. Commun. 236*, 651−654.
15. O'Reilly, M. S., Holmgren, L., Chen, C., and Folkman, J. (1996) *Nat. Med. 2*, 689−692.
16. Collen, D., Van Hoef, B., Schlott, B., Hartmann, M., Gührs, K.-H., and Lijnen, H. R. (1993) *Eur. J. Biochem. 216*, 307−314.
17. Lijnen, H. R., Van Hoef, B., and Collen, D. (1981) *Eur. J. Biochem. 120*, 149−154.
18. Lijnen, H. R., Lasters, I., Verstreken, M., Collen, D., and Jespers, L. (1994) *Anal. Biochem. 248*, 211−215.
19. Towbin, H., Staehelin, T., and Gordon, J. (1979) *Proc. Natl. Acad. Sci. U.S.A. 76*, 4350−4354.
20. Devereux, J., Haeberli, P., and Smithies, O. (1984) *Nucleic Acids Res. 12*, 387−395.
21. Niemann, S., Puehler, A., Tichy, H.-V., Simon, R., and Selbitschka, W. (1997) *J. Appl. Microbiol. 82*, 477−484.
22. Pitcher, D. G., Saunders, N. A., and Owen, R. J. (1989) *Lett. Appl. Microbiol. 8*, 151−156.
23. Ezaki, T., Hashimoto, Y., and Yabuuchi, E. (1989) *Int. J. Syst. Bacteriol. 39*, 224−229.
24. Friberger, P., and Knös, M. (1979) in *Chromogenic Peptide Substrates* (Scully, M. F., and Kakkar, V. V., Eds.) pp 128−140, Churchill Livingstone, Edinburgh.
25. Lucas, R., Holmgren, L., Garcia, I., Jimenez, B., Mandriota, S. J., Borlat, F., Sim, B. K., Wu, Z., Grau, G. E., Shing, Y., Soff, G. A., Bouck, N., and Pepper, M. S. (1998) *Blood 92*, 4730−4741.
26. Lasters, I., Van Herzeele, N., Lijnen H. R., Collen, D., and Jespers, L. (1997) *Eur. J. Biochem. 244*, 946−952.
27. Altschul, S. F., Madden, T. L., Schaffer, A. A., Zhang, J., Zhang, Z., Miller, W., and Lipman, D. J. (1997) *Nucleic Acids Res. 25*, 3389−3402.
28. Miles, L. A., Dahlberg, C. M., and Plow, E. F. (1988) *J. Biol. Chem. 263*, 11928−11934.
29. Sato, T. N. (1998) *Proc. Natl. Acad. Sci. U.S.A. 95*, 5843−5844.
30. Dong, Z., Kumar, R., Yang, X., and Fidler, I. J. (1997) *Cell 88*, 801−810.
31. Gately, S., Twardowski, P., Stack, M. S., Cundiff, D. L., Grella, D., Castellino, F. J., Enghild, J., Kwaan, H. C., Lee, F., Kramer, R. A., Volpert, O., Bouck, N., and Soff, G. A. (1997) *Proc. Natl. Acad. Sci. U.S.A. 94*, 10868−10872.
32. Stathakis, P., Fitzgerald, M., Matthias, L. J., Chesterman, C. N., and Hogg, P. J. (1997) *J. Biol. Chem. 272*, 20641−20645.
33. Lijnen, H. R., Ugwu, F., Bini, A., and Collen, D. (1998) *Biochemistry 37*, 4699−4702.
34. Patterson, B. C., and Sang, Q. A. (1997) *J. Biol. Chem. 272*, 28823−28825.

35. Friezner Degen, S. J., Bell, S. M., Schaefer, L. A., and Elliott, R. W. (1990) *Genomics 8*, 49−61.
36. Lottenberg, R., Minning-Wenz, D., and Boyle, M. D. P. (1994) *Trends Microbiol. 2*, 20−24.
37. Lottenberg, R. (1997) *Trends Microbiol. 5*, 466−467.
38. Boyle, M. D. P., and Lottenberg, R. (1997) *Thromb. Haemostasis 77*, 1−10.
39. Maeda, H., and Yamamato, T. (1996) *Biol. Chem. Hoppe-Seyler 377*, 217−226.

BI992014R